

## Influence of silica and black rice husk ash fillers on the diffusivity and solubility of gases in silicone rubbers

Luciane Sereda<sup>a,b</sup>, M. Mar López-González<sup>a</sup>, Leila L. Yuan Visconte<sup>b</sup>, Regina Célia R. Nunes<sup>b</sup>,  
Cristina Russi Guimarães Furtado<sup>c</sup>, Evaristo Riande<sup>a,\*</sup>

<sup>a</sup>*Instituto de Ciencia y Tecnología de Polímeros (CSIC), 28006 Madrid, Spain*

<sup>b</sup>*Instituto de Macromoléculas Professora Eloisa Mano, Universidade Federal do Rio de Janeiro, Brazil*

<sup>c</sup>*Grupo de Polímeros, Instituto de Química, Universidade do Estado de Rio de Janeiro, Brazil*

Received 2 December 2002; received in revised form 10 February 2003; accepted 13 February 2003

### Abstract

The preparation of elastomeric compositions based on poly(methylvinyl siloxane) using silica and rice husk ash as fillers is reported. Permeation of oxygen, nitrogen, carbon dioxide and methane across the compositions was measured in the temperature interval 30–60 °C under upstream pressures lying in the range 15–76 cm Hg. Permeation and diffusion coefficients were independent on the upstream pressure but both parameters were thermal activated processes described by the Arrhenius equation. It was found that the activation energy associated with the diffusion process is larger in the filled than in the unfilled rubbers. The results also showed that the fillers enhance gas solubility in polysiloxane compounds in such a way that in most situations the sorption process is exothermic. The analysis of the solubility and diffusivity of gases in the rubbers suggests very good adherence matrix-fillers that hinder micro-Brownian motions thus impeding the normal development of non-permanent holes through which the diffusive particles can easily jump. Neither the proportion nor the nature of the fillers alters the permselectivity characteristics of polysiloxane based compounds.

© 2003 Elsevier Science Ltd. All rights reserved.

**Keywords:** Gas transport; Silicone rubbers; Fillers-Rubber interaction

### 1. Introduction

The wide industrial use of polysiloxane rubbers arises from the combination of interesting properties presented by these elastomers that include excellent thermal and oxidative stability, good weatherability, good electric isolating properties, a wide interval of temperatures of use, resistance to oil, solvents, acids, fungi, etc. [1–5]. Another important aspect of these rubbers is the versatility of their synthesis processes that allows the incorporation of different chemical structures in the chains in proportion large enough to promote interesting changes in the properties of the elastomers [1–5]. For example, the random incorporation of vinyl groups in the chains facilitates the vulcanization process, preferentially carried out through these groups by means of peroxides.

In general, the mechanical properties of polysiloxane

elastomers are inferior to those of other organic elastomers, such as natural rubber. However, whereas the mechanical properties of polysiloxane elastomers only show a slight dependence on temperature, the properties of natural rubber and other elastomers undergo a great decrease with time at temperatures above 50 °C. In other words, polysiloxane elastomers exhibit better thermal properties than other organic ones [1,3]. Inorganic fillers are used to improve the mechanical properties of elastomers, and their reinforcement properties are larger the lower is the size of the filler particles and narrower the distribution of their sizes [6,7]. It is paramount to avoid the formation of filler agglomerates because they damage the mechanical properties of elastomers.

Inorganic fillers can be of natural and synthetic natures. Examples of the former are minerals, whereas carbon black and silica are examples of the latter. Silica obtained by precipitating sodium silicate in the presence of an acid or a salt of an alkali-earth metal is commonly used as reinforcing filler in rubbers. In this way, particles of diameter close to

\* Corresponding author. Tel.: +34-01-5622-900; fax: +34-91-5644-853.  
E-mail address: [riande@ictp.csic.es](mailto:riande@ictp.csic.es) (E. Riande).

the length of the chains in the extended conformation (0.01–0.05  $\mu\text{m}$ ) greatly improve the mechanical properties of rubbers [8–10]. Particles of lower size may form agglomerates that hinder a homogeneous dispersion of the filler in the composites.

An important issue in big rice producer countries, like Brazil, is the enormous disposal of rice husk. The burning process of this substance pollutes the environment with silica and therefore this is not the better way to get rid of the huge amounts of husk rice produced every year. White rice husk ash (WRHA) and black rice husk ash (BRHA) obtained from burning rice husk could in principle be used as reinforcing agents in a variety of rubbers. One of the first works on the use of rice husk as reinforcing filler in polymers was reported in 1975 by Haxo and Mehta [11], and the use of this filler in polypropylene was recently reported by Fuad and coworkers [12–14]. However, Ishak and Bakar [15] were the first workers who suggested the utilization of rice husk as rubber filler. In fact they used rice husk ash in the white (WRHA) and black (BRHA) varieties as reinforcing filler in elastomers, specifically, epoxidized natural rubber. They verified that the mechanical properties were inferior to those of composites prepared from commercial fillers, which was attributed to the relatively large size of the particle that only favors a moderate reinforcement. The use of rice husk ash as filler has also been used in SBR, EPDM and NR finding that the filler hardly alters the vulcanization process as well as the lifetime of these rubbers. Up to our knowledge, no work has been reported concerning the use of rice husk as filler for polysiloxane elastomers.

In our laboratories a study was undertaken that involves the preparation and characterization of rice husk ash, and the development of polysiloxane compositions using this product as reinforcing filler. An interesting characteristic of the resulting materials is their high permeability to gases. The permeability coefficient of polysiloxane can be two orders of magnitude larger than that of natural rubber. Introduction of lateral side groups into poly(1,1-dimethylsiloxane) may produce a significant alteration of the permeation and permselectivity of these materials. In spite of the amount of work carried out on the diffusivity of gases in polysiloxane materials [16,17], we are not aware of studies on the effect of the nature of fillers on the permeation properties of these compounds. The aim of this work was to investigate how BRHA affects gas transport in polysiloxane compounds. For example, it is interesting to investigate the presence of defects or voids in the matrix-filler interfaces that might facilitate gas transport. This would suggest a rather bad adherence of fillers to the polymer matrix. Elastomers filled with silica were also prepared and their permeation characteristics were determined and compared with those containing rice husk ash. These studies will provide information on the opacity of the different fillers to gas transport and also on the polymer-filler adherence.

## 2. Materials

Gross BRHA was provided by Empresa Brasileira de Pesquisa Agropecuária (EMBRAPA). This ash was used as received or after being grounded and sieved. The characteristics of these substances are given in Table 1.

Poly(methylvinylsiloxane) of density 1.08 g/cm<sup>3</sup> at 25 °C from Dow Corning do Brasil Ltda. The polymer contains 1 mol % of vinyl residues randomly distributed along the chains.

Silica (Zeoil 175) from Rhodia do Brasil SA. The characteristics of this filler are shown in Table 1.

2-5-Bis-tert-butyl-dimethylhexane peroxide (Varox) of density 0.87 g/cm<sup>3</sup> from Ipiranga Comércio e Química.

Gases of purity 5.0, supplied by Praxair, were used.

### 2.1. Granulometric analysis

The distribution of particle sizes of fillers was accomplished using the scanning electron microscopy (SEM) technique. For this purpose, samples of filler were pulverized onto appropriate metallic support, sputtering coated with a very thin layer of gold and placed into the vacuum chamber of the equipment. The analysis of the image obtained allowed the determination of the particle average size by using the computer program Global Lab. The average diameter of the particles was calculated by using the Rosin–Ramlet–Bennet model that requires the determination of the major axis of a high number of particles [18,19].

The results concerning the size of the particles used in this work are summarized in Table 1. In the same table other physical characteristics, such as specific area, density and pH, are also given. It can be seen that by grinding and sieving gross BRHA reduces the particle diameter in ca. 92%. The notation used for the sieved BRHA fillers is BRHA-MP. The calcination of BRHA-MP to yield calcined rice husk ash, denoted BRHA-C, promotes an increase in the particles size and therefore a reduction in the specific area. Photomicrographs of SC (standing for commercial silica), BRHA-MP and BRHA-C fillers are shown in Fig. 1.

### 2.2. Determination of fillers specific area

The specific area of the fillers was obtained from absorption of nitrogen at different partial pressures, at the temperature of liquid nitrogen [20]. The evaluation of the volume of the monolayers was obtained from the isotherms by using the Brunauer–Emmett–Teller (BET) equation given by

$$\frac{p}{V(p_0 - p)} = \frac{1}{V_m C} + \frac{C - 1}{V_m} \frac{p}{p_0} \quad (1)$$

where  $V$  is the adsorbed specific volume of nitrogen, in cm<sup>3</sup>/g, determined by a thermal conductivity detector,  $V_m$  is the specific volume (also in cm<sup>3</sup>/g) necessary to coat the

Table 1  
Physical characteristics of the fillers

Property	Commercial silica (SC)	Gross black rice husk ash (BRHA)	Ground and sieved black rice husk ash (BRHA-MP)	Calcined black rice husk ash (BRHA-C)
Average diameter of particles ( $\mu\text{m}$ )	10 (5–100) <sup>a</sup>	35	3.0	7.0
Specific area ( $\text{m}^2/\text{g}$ )	108 (185) <sup>a</sup>	74	139	106
Density ( $\text{g}/\text{cm}^3$ )	1.91 (2.0) <sup>a</sup>	1.10	1.95	2.24
PH	6.74 (6.50) <sup>a</sup>	9.26	8.98	10.14

<sup>a</sup> Quantities between brackets refer to values supplied by manufacturer.

particles of filler with a monolayer of nitrogen,  $p_0$  is the saturation pressure of liquid nitrogen in mm Hg,  $p$  is the reduced atmospheric pressure also in mm Hg, and  $C$  is a constant that depends on the heat of adsorption. From the plot of  $p/[V(p_0 - p)]$  against  $p/p_0$  a straight line is obtained and from the slope and intercept in the ordinate axis the  $V_m$  can be determined. Then the specific surface,  $A_{\text{sp}}$ , is calculated from the expression

$$A_{\text{sp}} = A_0 \frac{V_m}{M_a} \quad (2)$$

where  $A_0$  is the area covered by a mol of nitrogen in STP conditions, in  $\text{m}^2/\text{mol}$ , and  $M_a$  is the molar volume of the gas, in  $\text{cm}^3/\text{mol}$ .

In order to obtain good results it is necessary that the fillers-surface is completely dried. Therefore the fillers were kept at 150 °C for 24 h just before determining the adsorption isotherms.

### 2.3. Compounding process

Compounds containing 0, 10 and 30 g of silica or rice husk ash per one hundred g of poly(methylvinyl siloxane) (VMQ) were prepared in a roll mill with friction ratio of 1:1.25 at  $40 \pm 5$  °C. To all the compositions 0.8 g of crosslinking agent (Varox) per 100 g of polymer were added. The fillers were kept for 24 h in an oven at 120 °C, before being incorporated into the compounds. The compositions were analyzed on an oscillating disk rheometer with the aim of determining the vulcanization parameters, including the optimum cure time. The process employed to obtain the filled compositions included curing and post-curing. Thus the compounds were cured by compression molding at 170 °C and pressure of 3.0 MPa, in a Carver press for periods of time determined by the rheometric analysis. In order to complete the vulcanization step, the molded samples were subjected to a post-curing process at 200 °C in an oven provided with air circulation to eliminate the peroxide decomposition products. In this way

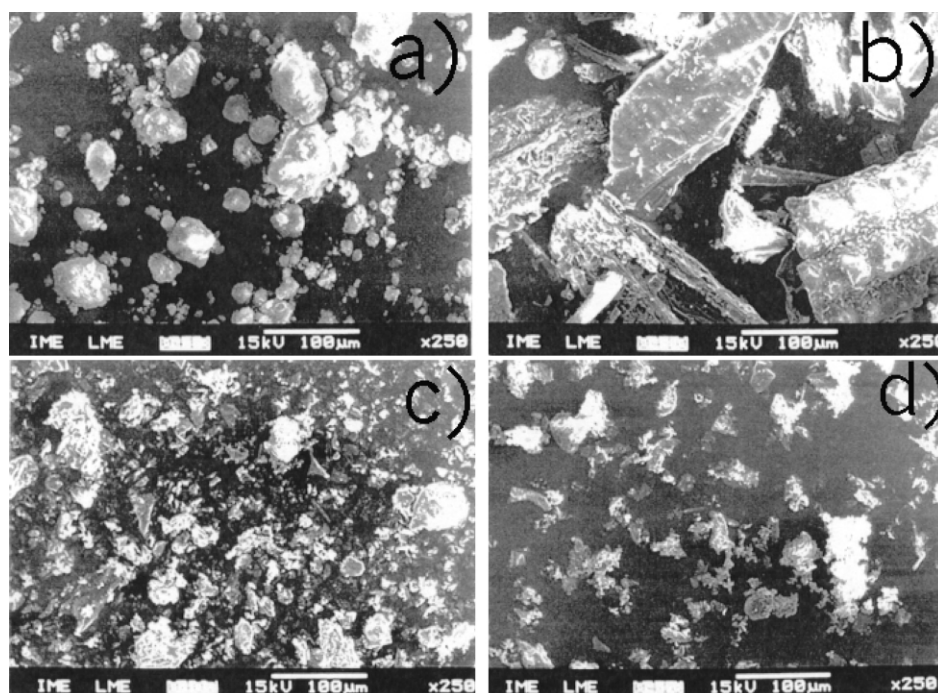


Fig. 1. Micrographies of (a) silica (SC), (b) gross black rice husk ash (BRHA), (c) sieved ground gross black rice husk ash (BRHA-MP), and (d) calcined sieved ground gross black rice husk ash (BRHA-C).

the following rubbers in sheet form were prepared: VMQ, VMQ-SC-10, VMQ-SC-30, VMQ-BRHA-MP-10, VMQ-BRHA-MP-30, VMQ-BRHA-C-10, VMQ-BRHA-C-30. Note that numbers in the notations indicate the amount of filler in g per 100 g of VMQ, or phr.

## 2.4. Permeation measurements

The experimental device used for permeation measurements is described in detail elsewhere [21]. Briefly, between two chambers equipped with pressure transducers circular rubber sheets of thickness 800–1700  $\mu\text{m}$  were placed. High vacuum was made in the two chambers and then gas, at a given pressure, was allowed to flow to the high pressure or upstream chamber. Gas diffusion from the upstream chamber to the low pressure or downstream chamber was monitored with a Leybold (0–10 torr) pressure transducer. Before each series of measurements, the system was vacuum calibrated by measuring the inlet of air into the downstream chamber. The experimental device was placed inside a thermostatic bath.

## 3. Results

The permeation of oxygen, nitrogen, carbon dioxide and methane was measured at different temperatures and different upstream pressures. Illustrative curves showing the variation of the pressure in the downstream chamber are shown in Fig. 2. The curves, that display a transitory at short times followed by a steady state region, are described by the expression [22]

$$p(t) = 0.2786 \frac{p_0 A L S T}{V} \times \left\{ \frac{D t}{L^2} - \frac{1}{6} - \frac{2}{\pi^2} \sum_{n=1}^{\infty} \frac{(-1)^n}{n^2} \exp\left(-\frac{n^2 \pi^2 D t}{L^2}\right) \right\} \quad (3)$$

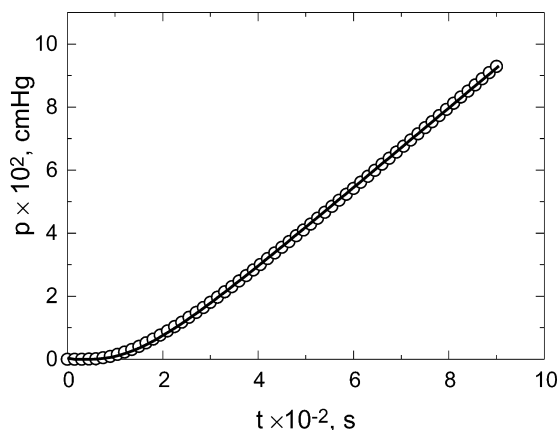


Fig. 2. Illustrative plot showing the variation of the pressure of nitrogen with time, at 30 °C and under the upstream pressure of 1 bar in VMQ-SC-10. Circles and continuous line indicate experimental and calculated values, respectively, the latter obtained by means of Eq. (3).

resulting from the integration of Fick's second law using appropriate boundary conditions [28]. In this equation  $p(t)$  and  $p_0$ , the pressures in the downstream and upstream chambers, respectively, are given in cm Hg,  $D$  and  $S$  are, respectively, the diffusion and solubility coefficients in  $\text{cm}^2/\text{s}$  and  $\text{cm}^3$  (STP)/( $\text{cm}^3$  cm Hg), and  $A$ ,  $L$  and  $V$  are, respectively, the area and thickness of the rubber-sheets and the volume of the downstream chamber in cgs units. In steady state conditions ( $t \rightarrow \infty$ ), Eq. (3) adopts the following form

$$p(t) = 0.2786 \frac{p_0 A L S T}{V} \left( \frac{D t}{L^2} - \frac{1}{6} \right) \quad (4)$$

According to this equation, the plot  $p(t)$  vs  $t$  is a straight line that intercepts the abscissa axis at a time  $\theta$ , called time lag, at which  $(D\theta/L^2) - 1/6 = 0$ . Therefore [23],

$$D = \frac{L^2}{6\theta} \quad (5)$$

By assuming that the permeability coefficient,  $P$ , is  $D$  times  $S$ , the value of  $P$  can be written as

$$P = 3.59 \frac{V L}{p_0 A T} \lim_{t \rightarrow \infty} \left( \frac{dp(t)}{dt} \right) \quad (6)$$

where  $P$  is given in barrers [ $1 \text{ barrer} = 10^{-10} \text{ cm}^3$  (STP)  $\text{cm}/(\text{cm}^2 \text{ s cm Hg})$ ]. From the values of  $P$  and  $D$ , obtained by the methods outlined above, the curves shown in Fig. 2 are obtained. It can be seen that Eq. (3) fits rather well to the experimental results even in the reinforced elastomers. The relative error involved in the determination of the diffusion coefficient by Eq. (5), estimated as

$$\Delta = \frac{100}{D} \left( \left| \frac{L \varepsilon(L)}{3\theta} \right| + \left| \frac{L^2 \varepsilon(\theta)}{6\theta^2} \right| \right) \quad (7)$$

was lower than 10%. An error lower than 6% was found for the permeability coefficient.

Values of the permeability coefficient in VMQ, VMQ-SC-10, VMQ-BRHA-MP-10 and VMQ-BRHA-C-10 are shown as a function of the upstream pressure in Fig. 3. For example, the value of  $P(\text{CO}_2)$  at 30 °C and  $p_0 = 76$  cm Hg decreases from 4090 barrers in VMQ to 2915, 2100, and 2130 barrers in VMQ-SC-10, VMQ-BRHA-MP-10 and VMQ-BRHA-C-10, respectively. Independently of the type of compositions, the permeability coefficients follow the trends  $P(\text{CO}_2) > P(\text{CH}_4) > P(\text{O}_2) > P(\text{N}_2)$ . It is noteworthy that  $P(\text{CO}_2)$  is nearly four times  $P(\text{CH}_4)$  in VMQ, but this factor decreases as the filler content increases. In some cases, the permeability coefficient seems to decrease slightly as the upstream pressure increases.

The results for the diffusion coefficient are plotted as a function of the upstream pressure in Fig. 4. In most cases the values of the diffusion coefficient follow the trends  $D(\text{O}_2) > D(\text{N}_2) > D(\text{CH}_4) \approx D(\text{CO}_2)$ , though the differences between them are moderate. Therefore solubility rather than diffusion must be responsible for the differences observed in the permeability coefficients.

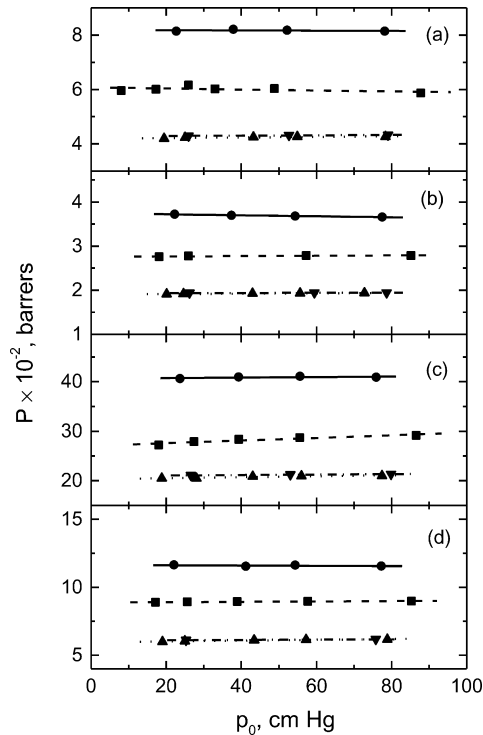


Fig. 3. Dependence of the permeability coefficient of O<sub>2</sub> (a), N<sub>2</sub> (b), CO<sub>2</sub> (c) and CH<sub>4</sub> (d) on the upstream pressure in VQM (●), VMQ-SC-10 (■), VMQ-BRHA-MP-10 (▲) and VMQ-BRHA-C-10 (▼).

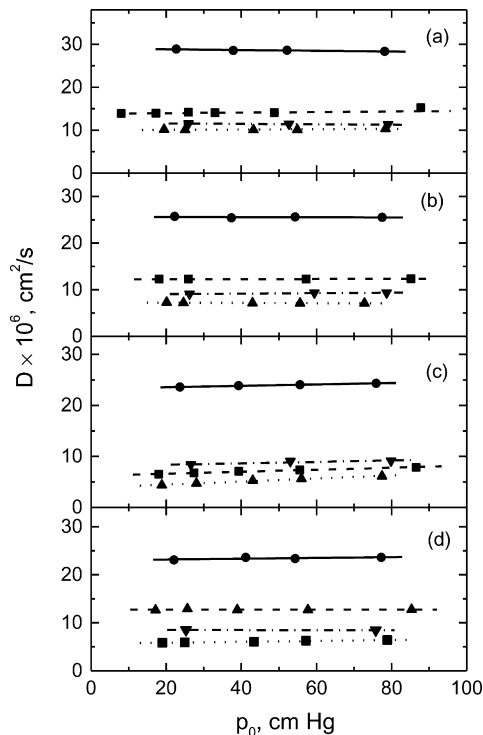


Fig. 4. Variation of the diffusion coefficient of O<sub>2</sub> (a), N<sub>2</sub> (b), CO<sub>2</sub> (c) and CH<sub>4</sub> (d) with the upstream pressure in VQM (●), VMQ-SC-10 (■), VMQ-BRHA-MP-10 (▲) and VMQ-BRHA-C-10 (▼).

The apparent solubility coefficient of CO<sub>2</sub> shows a strong dependence on the composition of the rubbers. Thus the value of  $10^3 S(\text{CO}_2)$  in  $\text{cm}^3(\text{STP})/(\text{cm}^3 \text{ cm Hg})$ , at 30 °C and  $p_0 = 76 \text{ cm Hg}$ , is ca. 17 in VMQ and the value of this quantity is nearly independent on the upstream pressure. In these rubbers  $S(\text{CH}_4) < (1/2)S(\text{CO}_2)$ . The solubility coefficient of carbon dioxide experiences a significant increase in the filled rubbers, though this increase depends on the fraction of fillers in the compositions. The values of  $10^3 S(\text{CO}_2)$  in VMQ-SC-10 and VMQ-SC-30 rubbers amount to 37 and 50  $\text{cm}^3/(\text{cm}^3 \text{ cm Hg})$ , respectively, at 30 °C and  $p_0 = 76 \text{ cm Hg}$ . Similar values are found for this parameter in VMQ-BRHA-MP-10 rubbers. The solubility coefficients of the other gases are less affected by the presence of fillers in the rubbers. In general,  $S(\text{CO}_2) > S(\text{CH}_4) > S(\text{O}_2) > S(\text{N}_2)$ .

#### 4. Discussion

Gas transport in membranes involves sorption of gas in the matrix, diffusivity of the penetrants across it and desorption on the other side of the membrane. Gas solubility in rubbery polymers can be obtained from the changes in free energy arising from mixing the gas in liquid form with the molecular chains. This approach leads to the following expression for the solubility coefficient [24,25]

$$\ln S = -\ln \bar{V}_A - (1 + \chi_A) + (1 + 2\chi_A)\bar{V}_A c_A - \frac{\lambda_{bA}}{RT_{bA}} \left(1 - \frac{T_{bA}}{T}\right) = \ln k_D + bc_A \quad (8)$$

where  $\bar{V}_A$  and  $c_A$  represent the partial molar volume and concentration of gas A in the polymer, respectively,  $\lambda_{bA}$  and  $T_{bA}$  are, respectively, the molar latent heat of evaporation and the boiling point of the penetrant and  $\chi_A$  is the enthalpic interaction parameter between the gas and the polymer. This expression reduces to Henry's law at low concentrations and deviates positively from it at high concentrations. According to Eq. (8), the more condensable is a gas, the higher its solubility coefficient in a polymer matrix is. The boiling point of the penetrants follows the trends  $T_b(\text{CO}_2) \gg T_b(\text{CH}_4) > T_b(\text{O}_2) > T_b(\text{N}_2)$  in consonance with the variation  $S(\text{CO}_2) \gg S(\text{CH}_4) > S(\text{O}_2) > S(\text{N}_2)$  experimentally observed. In rubbery barriers like these used in this study, solubility rather than diffusivity discriminates gas transport across polymers.

As we can see in Fig. 5, the variation of the solubility coefficient of gases in the filled silicone rubbers shows that SC and BRHA-MP fillers enhance this parameter, this enhancement specially being prominent for the most condensable gases. As for the calcined filler, its effect on gases solubility is less important. The presence of fillers could in principle facilitate gas adsorption on high potential surface points of the fillers. If this were the case, the apparent solubility coefficient should obey the following



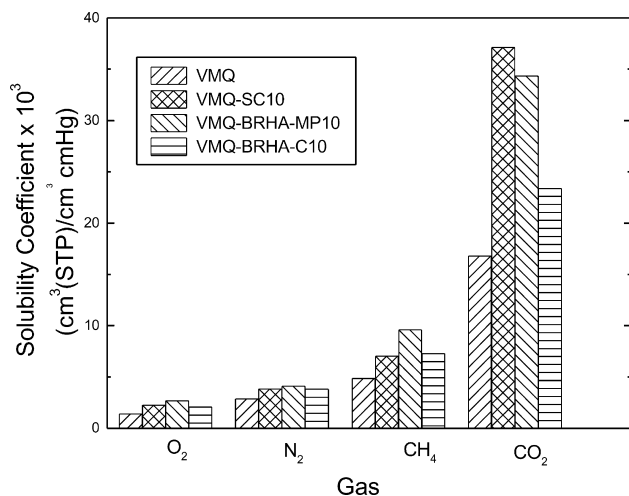


Fig. 5. Variation of the solubility coefficient of nitrogen, oxygen, methane and CO<sub>2</sub> in the four silicon membranes employed in this study.

equation [26]

$$S = k_D + \frac{C'_H b}{1 + bp} \quad (9)$$

According to the dual-mode model,  $k_D$  in Eq. (9) is the solubility Henry's law constant,  $C'_H$  is the adsorption gas concentration and  $b$  is an affinity parameter between the gas and the filler. The apparent constancy of the solubility coefficient with the variation of  $p_0$  seems to rule out adsorption processes at the fillers surface. Accordingly only absorption processes seem to take place in the reinforced elastomers.

In order to obtain the effect of the fillers on the heat of sorption, permeation experiments were conducted at several temperatures. It was observed that both the permeation and diffusion coefficients obey Arrhenius behavior as can be seen in Fig. 6 where, for illustrative purposes, plots representing the natural logarithm of these magnitudes against the reciprocal of the absolute temperature are shown. Accordingly, the temperature dependence of  $P$  and  $D$  can be written as

$$P = P_0 \exp\left(-\frac{E_P}{RT}\right), \quad D = D_0 \exp\left(-\frac{E_D}{RT}\right) \quad (10)$$

where  $P_0$  and  $D_0$  are pre-exponential factors whereas  $E_P$  and  $E_D$  are, respectively, the activation energies associated with the permeation and diffusive processes. On the other hand, by assuming that  $S = P/D$ , the temperature dependence of the solubility coefficient is given by

$$S = S_0 \exp\left(-\frac{\Delta H_s}{RT}\right) = \frac{P_0}{D_0} \exp\left(-\frac{E_P - E_D}{RT}\right) \quad (11)$$

where  $S_0$  is a pre-exponential factor and  $\Delta H_s$  is the heat of sorption. According to this expression, the heat of sorption is related to the activation energies of the permeation and

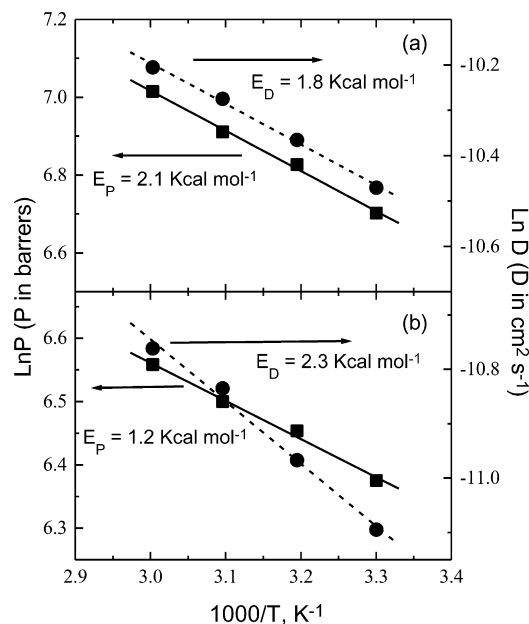


Fig. 6. Illustrative Arrhenius plots of the permeability and diffusion coefficients of oxygen in VMQ (a) and VMQ-SC-10 (b) at  $p_0 = 76$  cm Hg.

diffusive processes by

$$\Delta H_s = E_P - E_D \quad (12)$$

The values of the activation energies associated with the permeability and diffusion coefficients as well as the heats of sorption for different gases in the unfilled and filled rubbers are collected in Figs. 7–10. Note that these results are plotted for two upstream pressures, 22.8 and 76 cm Hg. It can be seen that in all cases the upstream pressure has a minor incidence on the activation energies of the different steps of the permeation process.

The activation energies associated with the permeability coefficient in unfilled silicone rubbers are positive for all gases with exception of carbon dioxide that is slightly negative. This means that the heat of sorption overcomes the activation energy of the diffusive process. Therefore the

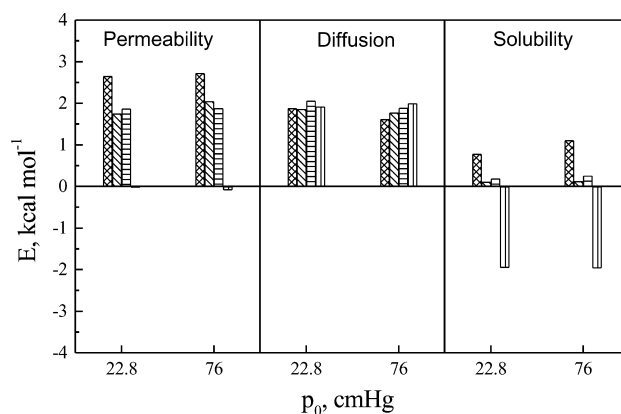


Fig. 7. Activation energies for the permeability and diffusion coefficients as well as heat of sorption for N<sub>2</sub> (diagonal lines), O<sub>2</sub> (cross-hatch), CH<sub>4</sub> (horizontal lines) and CO<sub>2</sub> (vertical lines) in VMQ.

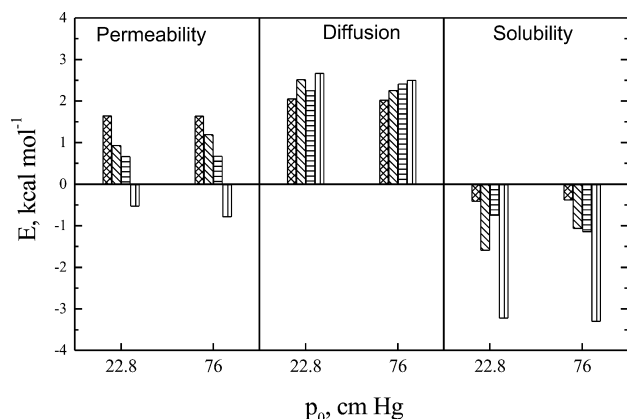


Fig. 8. Activation energies for the permeability and diffusion coefficients as well as heat of sorption for  $N_2$  (▨),  $O_2$  (▧),  $CH_4$  (▩) and  $CO_2$  (▪) in VMQ-SC-10.

solubility of  $CO_2$  in VMQ is an exothermic process and as result the solubility of this gas decreases with increasing temperature. For the other gases  $E_p > E_D$  as occurs with  $N_2$  or they are rather similar as happens with  $CH_4$  and  $O_2$ .

A dramatic change occurs in the heats of sorption in the filled rubbers. If the values of  $\Delta H_s$  for VMQ-SC-10 are compared with those of VMQ-BRHA-MP-10, no significant differences are observed. For example, in both cases  $E_p(CO_2) < 0$  and the solubility of all gases in these filled elastomers is an exothermic process. The absolute values of the heat of sorption follow the trends  $|\Delta H_s(CO_2)| > |\Delta H_s(CH_4)| > |\Delta H_s(O_2)| > |\Delta H_s(N_2)|$ . It is worth noting that the absolute values of the heat of sorption of these gases are slightly lower in VMQ-SC-10 than in BRHA-MP-10. With the exception of  $CO_2$ ,  $E_D > |\Delta H_s|$  and, as a consequence, the permeation of nitrogen, oxygen and methane increases with increasing temperature.

By comparing the heat of sorption for  $CO_2$  in elastomers containing 30 phr of fillers one can see that  $|\Delta H_s|(VMQ-SC) > |\Delta H_s|(VMQ-BRHA-C) > |\Delta H_s|(VMQ-BRHA-MP)$ . The solubility of  $CH_4$  and  $N_2$  in VMQ-SC and VMQ-BRHA-MP-30 is an endothermic process, whereas a process of this

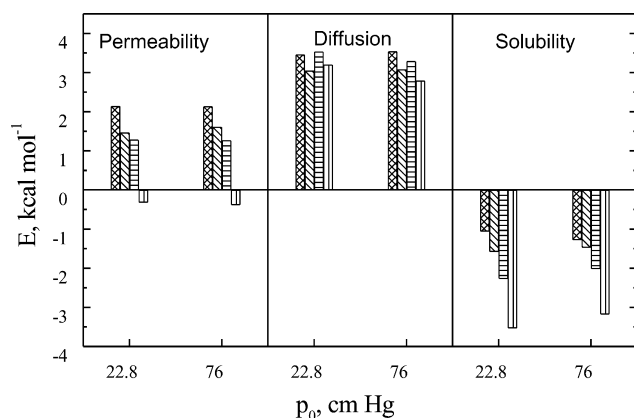


Fig. 9. Activation energies for the permeability and diffusion coefficients as well as heat of sorption for  $N_2$  (▨),  $O_2$  (▧),  $CH_4$  (▩) and  $CO_2$  (▪) in VMQ-BRHA-MP-10.

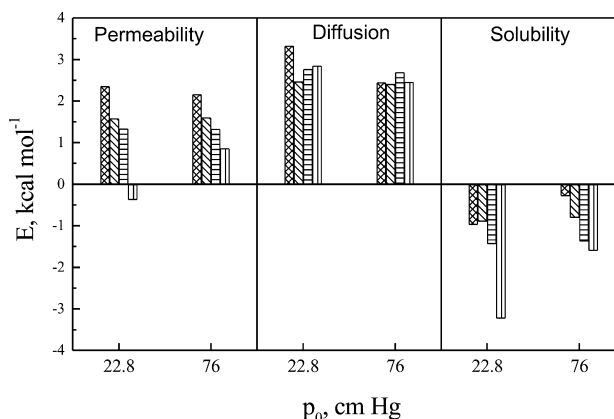


Fig. 10. Activation energies for the permeability and diffusion coefficients as well as heat of sorption for  $N_2$  (▨),  $O_2$  (▧),  $CH_4$  (▩) and  $CO_2$  (▪) in VMQ-BRHA-C-10.

type occurs for  $CH_4$  in VMQ-BRHA-MP. In the other cases the solubility of gases is an exothermic process.

A significant increase in the activation energies associated with the diffusive process is observed when the values of  $E_D$  in elastomers with 10 phr of fillers are compared with those of VMQ. On the other hand, the permeability coefficient of the filled samples is lower than the volume fraction of polymer in the filled sample times the permeability coefficient of VMQ. These facts suggest the absence of voids that might facilitate the diffusive process. Therefore the fillers show a high compatibility with the poly(vinylmethyl siloxane) matrices in such a way that the polymer-fillers interface greatly hinders the diffusive processes. This fact is reflected in the study of the mechanical properties of these elastomers.

Gas permselectivity of a gas A with respect to another, B, is defined as

$$\alpha(A/B) = \frac{P(A)}{P(B)} = \frac{S(A)}{S(B)} \frac{D(A)}{D(B)} \quad (13)$$

A summary of the values of the permselectivity coefficients of different gases at 30 °C and two upstream pressures are shown in Table 2. With the exception of  $\alpha(CO_2/N_2)$  whose values are in the vicinity of 10, the results for  $\alpha(CO_2/CH_4)$ ,  $\alpha(CH_4/N_2)$  and  $\alpha(O_2/N_2)$  lie in the interval 2–3. In general the fillers do not affect the selectivity characteristics of the elastomers and also, with the exception of  $\alpha(CO_2/N_2)$ , the temperature has a minor effect on the permselectivity of the other gases. Thus by increasing the temperature from 30 to 60 °C,  $\alpha(CO_2/N_2)$  in VMQ, at  $p_0 = 76$  cm Hg, decreases from 11.18 to 7.31. This change, for example, is only from 2.22 to 2.01 for  $\alpha(O_2/N_2)$ .

Owing to the micro-Brownian motion of polymers in the rubbery state, non-permanent holes are continuously being created through which the molecules of diffusant can easily jump. In principle, the dependence of the diffusion

Table 2  
Permselectivity coefficients of reinforced fillers at 30 °C and two upstream pressures

Composition	$p_0$ (cm Hg)	$\alpha(\text{CO}_2/\text{CH}_4)$	$\alpha(\text{CO}_2/\text{N}_2)$	$\alpha(\text{CH}_4/\text{N}_2)$	$\alpha(\text{O}_2/\text{N}_2)$
VMQ	22.8	3.49	10.91	3.12	2.19
	76	3.54	11.18	3.12	2.22
VMQ-SC-10	22.8	3.12	10.04	3.22	2.22
	76	3.25	10.46	3.22	2.10
VMQ-SC-30	22.8	2.97	10.05	3.45	2.42
	76	3.06	10.38	3.45	2.30
VMQ-BRHA-MP-10	22.8	3.42	10.70	3.13	2.20
	76	3.40	10.82	3.18	2.20
VMQ-BRHA-MP-30	22.8	3.22	10.18	2.63	2.15
	76	3.62	10.46	2.89	2.21
VMQ-BRHA-C-10	22.8	3.40	10.68	3.23	2.20
	76	3.40	10.84	3.23	2.20
VMQ-BRHA-C-30	22.8	3.39	10.76	3.23	2.21
	76	3.41	10.83	3.23	2.19

coefficient on the free volume can be written as [27–30]

$$D = RTA_D \exp\left(-\frac{B}{v_f}\right) \quad (14)$$

where  $A_D$  is a pre-exponential function,  $v_f$  is the fractional free volume and  $B$  is a parameter that is the ratio of the critical volume necessary for a jump of the diffusant to a neighbor hole to take place to the volume of the segments involved in the formation of a hole. The free volume with respect to a temperature  $T_0$  and pressure  $p_0$  of reference is given by [31,32]

$$v(p, T) = v(p_0, T_0) + \alpha_f(T - T_0) - \beta(p - p_0) + \gamma\phi_A \quad (15)$$

where  $\alpha_f = [(1/v)\partial v/\partial T]$  is the normalized volume expansion coefficient,  $\beta = [(1/v)\partial v/\partial p]$  is the compression coefficient and  $\gamma = [(1/v)\partial v/\partial \phi_A]$  accounts for the penetrant concentration changing the free volume. By substituting Eq. (15) into Eq. (14) the following expression relating the diffusion coefficient with the upstream pressure is obtained

$$\frac{1}{\ln(D_0/D)} = \frac{v(T_g, 76) + \alpha_f(T - T_g) - \beta(p - 76)}{B} \quad (16)$$

where  $D_0 = RTA_D$  and the last term in Eq. (15) was neglected. By taking [33]  $v(T_g, 76) = 0.071$  and considering that  $\alpha_f = 10.3 \times 10^{-4} \text{ K}^{-1}$ , the values of  $D_0$  and  $B$  at 30 °C were obtained from plots of Eq. (16) in isobaric conditions. Then from the plots of  $1/\ln(D_0/D)$  against  $p - 76$ , the value of  $\beta/B$  was determined. Results for  $B$  and  $\beta$  using  $\text{CO}_2$  as diffusant were 0.38 and  $1.48 \times 10^{-8} \text{ cm}^2/\text{dyne}$ . This value of  $\beta$  is significantly higher than that found using this same analysis for natural rubber, as one would expect taking into account the higher free volume of polydimethyl siloxane. The value of the compressibility coefficient slightly decreases as the fillers content increases. A thorough analysis about the determination of compressibility using the technique outlined above would require performing permeation experiments over a wider interval of pressures.

## 5. Conclusions

In general silica and sieved ground BRHA fillers enhance the solubility of gases in VMQ elastomers in such a way that the sorption of most gases in these composites is a highly exothermic process, at least for the composites with 10 phr of fillers content. However, fillers decrease the diffusivity in such a way that the permeability coefficient in the reinforced elastomers is smaller than the volume fraction of polymer in the filled samples times the permeation in unfilled VMQ elastomers. This behavior suggests a good dispersion of fillers in poly(methylvinyl siloxane) that enhance the solubility of the gases in the polymer-filler interfaces, and also the absence of voids in the interface that would promote gas diffusivity in the reinforced elastomers. Good adherence of the fillers to the polymer matrix presumably hinders micro-Brownian motions thus severely reducing the formation of non-permanent holes that promote diffusivity processes. Therefore it is expected that these fillers greatly improve the mechanical properties of the filled elastomers.

Fillers do not alter the permselectivity characteristics of poly(methylvinyl siloxane) composites.

## Acknowledgements

The authors are indebted to CAPES (Coordenação de Aperfeiçoamento de Pessoal de Nível Superior) for financial support to one of us (LS), to Dow Corning and Rhodia do Brazil for providing, respectively, the polysiloxane rubber and the commercial silica. Support from the CAM (PGE 2000), CSIC and CNPq is also gratefully acknowledged.

## References

- [1] Blow CM. In: Blow CM, editor. Rubber technology. Silicone



- rubbers—SI, London: Institution of Rubber Industry; 1971. p. 130–54. Chap. 4.
- [2] Hardaman B, Torkelson A. In: Mark H, Bikales NM, Overberg CG, Menges G, editors. *Silicones. Encyclopedia of polymer science and engineering: silicones*, vol. 15. New York: Wiley; 1986. p. 204–308.
  - [3] Caprino JC, Maconder RF. In: Morton M, editor. *Silicone rubber. Rubber technology: silicone rubber*, New York: Van Nostrand Reinhold; 1987. p. 375–409. Chap. 13.
  - [4] Palmanter KE. In: Browmick AK, Stephens HL, editors. *Advances in silicone rubber technology. Handbook of elastomers—new developments and technology: advances in silicone rubber technology*, New York: Marcel Dekker, Inc; 1988. p. 551–615. Chap. 17.
  - [5] Brydson JA. *Silicone rubber. Rubber materials and their compounds*, London: Elsevier Applied Science; 1988. Chap. 13, p. 254–70.
  - [6] Boonstra BB. In: Blow CM, editor. *Reinforcement by fillers. Rubber technology and manufacture*, London: Butterworths; 1971. p. 269–308. Chap. 7.
  - [7] Hepburn C. *Rubber compounding ingredients—need, theory, and innovation. Part I. Vulcanizing systems, antidegradants, and particulate fillers for general purpose rubbers. Rapra review reports. Rapra Technology Ltd, report 79. 7(7); 1994. p. 1–7.*
  - [8] Horn JB. In: Blow CM, editor. *Materials for compounding and reinforcement. Rubber and technology*, London: Institution of the Rubber Industry; 1971. p. 202–18. Chap. 6.
  - [9] Ferch H, Toussaint HE. *Kautsch Gummi Kunst* 1996;49:589.
  - [10] Boonstra BB, Cochrane H, Dannenberg EM. *Rubber Chem Technol* 1975;48:556.
  - [11] Haxo HE, Mehta PK. *Rubber Chem Technol* 1975;48:71.
  - [12] Ahmad Fuad MY, Ismail Z, Mansor MS, Mohd Ishak Z, Mohd Omar K. *Polym J* 1995;27:1002.
  - [13] Ahmad Fuad MY, Yaakov I, Mohd Ishak Z, Mohd Omar K. *J Appl Polym Sci* 1995;56:1557.
  - [14] Ahmad Fuad MY, Yaakov I, Mohd Ishak Z, Mohd Omar K. *Eur Polym J* 1995;31:885.
  - [15] Mohd Ishak Z, Bakar AA. *Eur Polym J* 1995;31:259.
  - [16] Stern SA, Shah VM, Hardy BJ. *J Polym Sci: Part B: Polym Phys* 1987; 25:1263.
  - [17] Stern SA. *J Memb Sci* 1994;94:1.
  - [18] Sawyer C, Grubb DT. *Polymer microscopy*. London: Chapman & Hall; 1987. Chap 1, p. 1–15.
  - [19] Targer A. *Physical chemistry of polymers*. Moscow: Mir; 1978. Chap. 16, p. 493–98.
  - [20] ASTM D. 3037-86—Standard Test Method for Carbon Black-Surface Area by Nitrogen, American Society for Testing and Materials, Section 9, vol. I, Philadelphia; 1986.
  - [21] Compañ V, Andreu A, López ML, Alvarez C, Riande E. *Macromolecules* 1992;30:6984.
  - [22] Crank J. *The mathematics of diffusion*. Oxford: Oxford University Press; 1975.
  - [23] Barrer RM. *Trans Faraday Soc* 1939;35:628.
  - [24] Flory PJ. *Principles of chemistry*. Ithaca, NY: Cornell University Press; 1953.
  - [25] Petropolis JH. *Pure Appl Chem* 1993;65(2):219.
  - [26] Kesting RE, Fritzsche AK. *Polymeric gas separation membranes*. New York: Wiley-Interscience; 1993. p. 32.
  - [27] Fujita H. In: Crank J, Park G, editors. *Organic vapors above the glass transition temperature. Diffusion in polymers*, New York: Academic Press; 1968. p. 75–105.
  - [28] Stern SA, Fang SM, Frisch HL. *J Polym Sci Part A-2* 1972;10:201.
  - [29] Stern SA, Fang SM, Frisch HL. *Chem Eng Sci* 1975;30:773.
  - [30] Reis-Nunes RC, Compañ V, Riande EJ. *Polym Sci: Part B: Polym Phys* 2000;38:393.
  - [31] Kulkarni SS, Stern SA. *J Polym Sci: Polym Phys Ed* 1983;21:467.
  - [32] Stern SA, Sampat SR, Kulkarni SS. *J Polym Sci: Polym Phys Ed* 1986;24:2149.
  - [33] Ferry JD. *Viscoelastic properties of polymers*. New York: Interscience; 1970. p. 316.